Sub-10-attosecond Fibre-length Stabilisation using Phase-locked Spectral Interferometry

Jack Morse[1,3], Pedro Oliveira[1*], Alexander Aiken[2], Marco Galimberti[1]

[1*]Central Laser Facility, STFC, Rutherford Appleton Laboratory, Harwell, OX11 0QX, United Kingdom.
[2]Accelerator Science and Technology Centre (ASTeC), STFC, Daresbury Laboratory, Warrington, WA4 4AD, United Kingdom.
[3]University of Bath, Claverton Down, Bath, BA2 7AY, United Kingdom.

*Corresponding author(s). E-mail(s): pedro.oliveira@stfc.ac.uk;
Contributing authors: jack.morse2001@gmail.com; alexander.aiken@stfc.ac.uk;
marco.galimberti@stfc.ac.uk;

Abstract

We present a new proof-of-principle linear technique for attosecond-level fibre length stabilisation. Key advantages of this technique include minimal light requirements, spectral phase independence, versatile light source compatibility, cost-efficiency, robustness to intensity variations, a reasonable tolerance to path difference and zero-timing monitoring. We envision that this could be implemented in large-scale science facilities such as complex high power lasers and accelerators. This method offers unprecedented precision, with drift-free operation tested over 24 hours and total timing jitter reduced to a remarkable 6.8 attoseconds up to the Nyquist frequency with an average power of 25 μW. The sensitivity of the system has been characterised to 91.91 mV/fs.

Keywords: Spectral interferometry, Timing, Synchronisation, Fibre link

1 Introduction

In the realm of ultrafast sciences, achieving low-jitter femtosecond-level control over optical paths and fibre lengths is a paramount objective. The implications of such precision extend far and wide, particularly within the domains of many world-leading large-scale science facilities, including particle accelerators, laser facilities and next-generation X-ray free electron lasers (XFELs) [1, 2].

An important possible application of this technique will be the new laser facilities, where several femtosecond lasers are combined in the same target area with desires for femtosecond delays between them. Such forthcoming examples are for instance Vulcan 20-20 [3] or ELI facilities [4], which will have several petawatt (PW) level ultrafast lasers with their arrival time precisely controlled in a target chamber. Other science facilities, like the MEC LCLS [5] upgrade and CLARA-FEBE, will have high intensity lasers combined with other sources of coherent light – this will make such developments mandatory in the medium term.

The primary method for stabilising fibre links is currently the balanced optical cross-correlator

(BOXC). These systems have been able to stabilise path lengths down to 200 attoseconds [6], albeit with larger path lengths of the order of 1 km. However, these systems imply the use of ultra-stabilised oscillators and dispersion compensated fibres, neither of which are required for this system.

Here we present a novel approach involving phase-locking a spectral interferogram. As spectral interferometry is a linear process, it has a few advantages over other methods. Firstly, the technique can be used with low powers unlike methods involving nonlinear crystals, where away from saturation the detection signal has a nonlinear dependence on intensity. As a zero-crossing technique (like BOXCs) it is insensitive to small intensity variations. Furthermore, this technique has fewer restrictions on the laser source, and in reality a super-luminescence diode (SLD) or amplified spontaneous emission (ASE) source would be enough with no laser required. The stability of the frequency of the pulse train is also not essential as the same pulse from the oscillator is compared each time.

We use off-the-shelf components to construct an in-fibre Michelson interferometer. What we ultimately lock is the difference in fibre path length between the two arms. The difference in length between the fibres is an important factor, but this method should be capable of working even if the fibre lengths differ by up to a couple meters.

This method also overcomes another challenge faced by many methods: that of relocating zero-timing once it has been lost. For processes involving direct overlap of two pulses, the intensity of the detection signal is proportional to the delay between them but approaches zero outside a small region of intersection, approximately equal to the sum of the FWHMs of the pulses being correlated. However, as spectral interferometry can occur away from direct overlap, and as the pulses are not required to be short, this region is not only capable of being much larger, but the commercial spectrometer can monitor the zero delay wavelength (ZDW) in the spectrum with a range of tens of picoseconds. This gives knowledge of which direction and how far to change the delay to shift the ZDW back to the centre of the window.

In the following sections we present the method, along with the necessary calibrations, the experimental setup, and in the results section we present our long and short term stabilisation results.

2 Methods

As shown schematically in Fig. 1, we split a laser beam in two, with approximately half traversing a reference fibre and the remainder travelling through an adjustable transport fibre containing a stepper motor for rough timing adjustment, an in-line fibre stretcher (FS) for fast delay compensation and a voice coil (M1) to adjust for slow drifts; both fibres were of the same type (HI1060 single mode (SM)) and a mirror is placed in the retro position at the end of each fibre to double pass the system. Both fibres were in reality next to each other on an optical table, but we envision the reference fibre being kept in a temperature, humidity and vibration controlled environment.

Both sides of the interferometer have nominally the same total fibre propagation of 70 m with an uncertainty of 1%. The output is divided by a polarisation beam-splitter and the resulting pulse enters two different spectrometers – a commercial spectrometer and a home-built fast spectrometer which uses a position sensor device (PSD) as a detector. The commercial spectrometer gives us the range for monitoring purposes whilst the fast spectrometer signal was used in a PID loop to lock the delay between the pulses by moving a fibre stretcher in the adjustable fibre. The grating G1 is imaged at a line focus onto first a camera with a 7 nm field of view (FOV) for alignment purposes, and second the PSD with a 2 nm FOV which is equal to the size of the fringe we chose to lock to. The laser used was a 1040 nm-centered 20 nm bandwidth 80 MHz source.

In order to establish the theory for this we constructed a model considering a small difference in the refractive indices between each arm of the interferometer (Δn_f). Due to the fact that the difference in path lengths between the two arms substantially smaller than the length of both arms we introduced a term in our spectral phase that accounts for differences in refractive index between the two arms. The spectral interference seen between the recombined pulses is given in

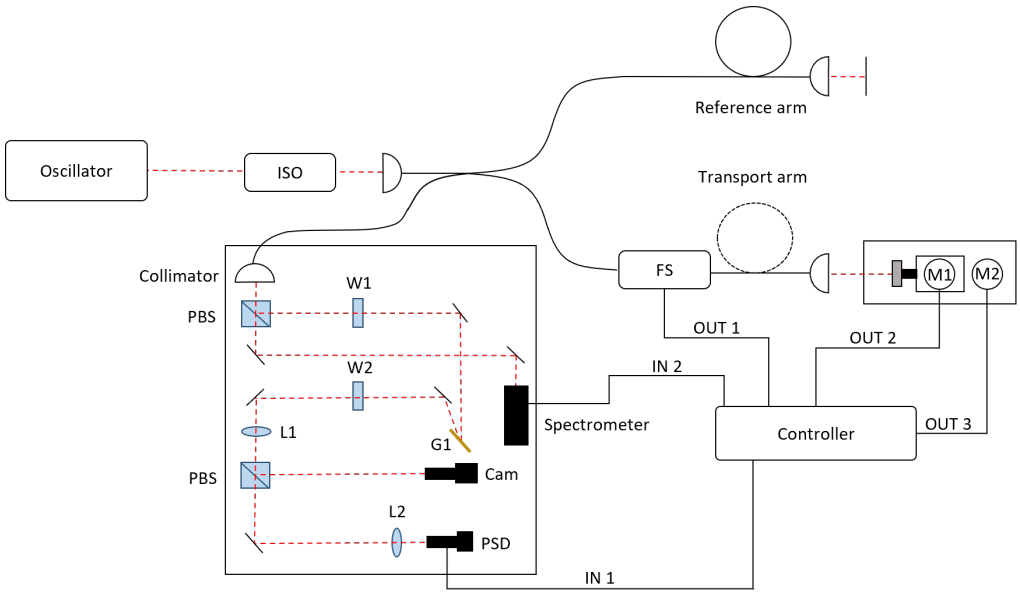

Fig. 1: Experimental setup. W1 and W2 are $\lambda/4$ waveplates; G1 is a 1200 lines/mm reflective diffraction grating; L1 a +150 mm lens; L2 a +25.4 mm lens; FS is the fibre stretcher; M1 a voice coil actuator; M2 a stepper motor; PSD a position sensing device, ISO is an optical Faraday isolator, PBS is a polarisation beam-splitter.

general by

$$S(\lambda) = \left(|E(\lambda)| \cos\left(\frac{\Delta\varphi(\lambda)}{2} \right) \right)^2 \qquad (1)$$

where the spectral phase difference $\Delta\varphi$ depends on the delays in air and the two fibres separately:

$$\Delta\varphi = \frac{2\pi}{\lambda} \left(\Delta L_f \overline{n}_f + \overline{L}_f \Delta n_f + \Delta L_{air} \right), \qquad (2)$$

with $\overline{L}_f$ being the mean fibre path length between the two arms and ΔL_f and ΔL_{air} representing the difference in fibre and air between the transport and reference arms respectively. The ZDW by definition exists when the delay between a single wavelength in each pulse is zero. In our set-up the spectral phase difference was approximately quadratic and so there was only a single ZDW in the observed spectral interference, which occurred at $\lambda = \lambda_0$ when $d\Delta\varphi/d\lambda = 0$. Thus, when this condition is satisfied

$$\Delta L_{air} = -\Delta L_f \overline{n}_g - \overline{L}_f \Delta n_g. \qquad (3)$$

The group delay dispersion (GDD) of the whole setup when the ZDW is the central wavelength, is by definition equal to the second derivative of the phase with respect to ω at this angular frequency. For our system $\partial^2\varphi/\partial\lambda^2$ had a value of 0.27852 rad nm^{-2} and was extracted from the spectrum. The analytical form of this is

$$\frac{\partial^2 \Delta\varphi}{\partial\lambda^2} = \frac{2\pi}{\lambda} \left(\frac{\partial^2 \overline{n}_f}{\partial\lambda^2} \Delta L_f + \frac{\partial^2 \Delta n_f}{\partial\lambda^2} \overline{L}_f \right) \qquad (4)$$

in terms of the fibre lengths, which is valid at the condition of λ being the ZDW. This yields an experimental GDD of 91.7×10^3 fs^2.

We express the phase as a quadratic polynomial written as:

$$\Delta\varphi \simeq \beta(\lambda - \lambda_0)^2 + \delta \qquad (5)$$

where λ_0 is the ZDW and β is the total difference in GDD between the two arms: these were two parameters we could detect in our experiment. By introducing an incremental phase attributed to a incremental time difference of $d\tau$ we obtained the variation in these two parameters is given in Eq.

6 and 7:

$$\frac{d\lambda_0}{d\tau} = \frac{\pi c}{\lambda_0^2}\left(\frac{d^2\Delta\varphi}{d\lambda^2}\right)^{-1}, \tag{6}$$

$$\frac{d\Delta\varphi}{d\tau} = \frac{2\pi c}{\lambda_0}. \tag{7}$$

The expected interference spectrum was then modelled using Eq. 1 and the measured GDD. Fig. 2 shows the agreement between the measured dispersion value and the actual setup.

Stabilisation Scheme

Fringe locking was achieved through a two-level PID feedback loop which was tuned [7], with the output voltage of the first loop being split with one part amplified and sent to the FS and the other part becoming the input to the second PID loop, with its output being sent to M1. The PSD in the first (fast) loop works by outputting a voltage which is scaled by a sum value, which is proportional to the total light on the sensor – the model used was a PDP90A (more information can be found on Thorlabs' website). The fibre stretcher had a range of around 14 μm but with a quoted bandwidth of 150 kHz, whereas the voice coil can compensate a much larger range of delays (up to 20 picoseconds) with a bandwidth of around 1kHz. The voice coil device also has a known resonance line at around 25 Hz, but future planning can mitigate the effect of this. The second loop compensates for larger but slower delays by always keeping the output of the first loop around zero. Although we didn't find it necessary, a third PID loop could be implemented if required to centre the second actuator around zero, potentially increasing its response speed and the temporal range.

Calibration

To assess the performance of our system and conduct calibration, we employed two distinct approaches, one for each spectrometer. For the slow spectrometer, we applied a Hilbert transform to detect both the upper and lower envelopes, followed by a minimisation algorithm designed to fit the parabolic phase, as described in Eq. 5. With this we obtained Fig. 2 and the coefficients of Eq. 5; the GDD of the system came out at $\beta = 0.27852$ rad nm^{-2}.

To quantify larger delay variations, we introduced a known delay, τ. According to Eq. 6, this delay should result in a shift in the ZDW location of 3.1 nm/ps. In practice we adjusted the motor M2 in micrometer increments while monitoring the change in the ZDW location with the stabilisation loops turned off. This calibration process, illustrated in Fig. 3, yielded a value of 2.8 nm/ps, closely aligning with our calculated expectation.

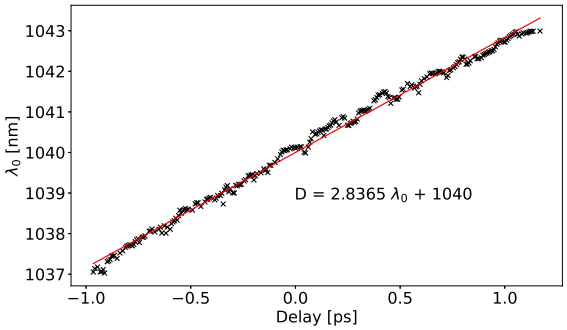

Fig. 3: Change in location of ZDW (λ_0) as the delay is changed by varying M2 in micrometer steps. The relation is linear and shows the change in ZDW in the spectrum with respect to time $d\lambda_0/dt = 2.8365$ nm/ps.

For the second spectrometer we can detect the fast variations in the form of a voltage derived from the PSD, this is a spectral phase measurement. From the theory set out in Eq. 7, the instantaneous spectral phase difference evaluated at the ZDW can be related to a phase delay where a change in phase of 2π directly corresponds to a phase delay of T, the optical period of the ZDW, between the two pulses. To determine the system's sensitivity, we measured the phase change in the spectrum observed by the slow spectrometer. This measurement was conducted while adjusting the set-point of the fast loop within a range of –30 mV to +30 mV. Throughout this adjustment, we maintained the lock to a selected fringe. The system would mainly be changing the fibre stretcher. An example of the spectra observed in this experiment as well as the calibration betwen delay and voltage of the fast spectrometer can be seen in Fig.4. A calibration of 10.9 as/mV was obtained, which directly corresponds to a sensitivity of 91.91 mV/fs. This result

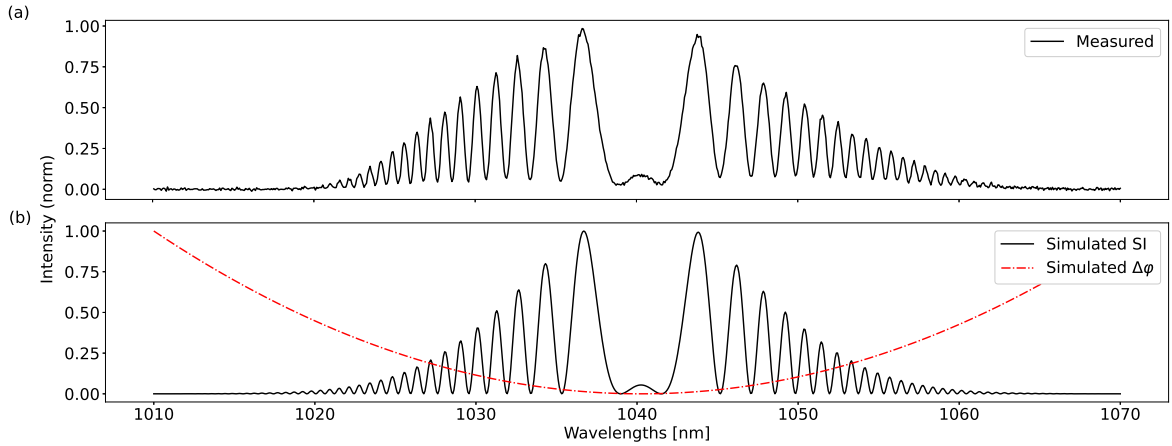

Fig. 2: (a) Measured spectral interference compared with (b) the simulated interference of two Gaussian pulses of equal intensity with 10 nm bandwidth and $\Delta\varphi = 0.27852\ [\mathrm{nm}^{-2}] \cdot(\lambda - 1040.2\ [\mathrm{nm}])^2 + 2.7$ rad.

is an order of magnitude more than practically measured in comparable systems using balanced cross-correlator methods [8].

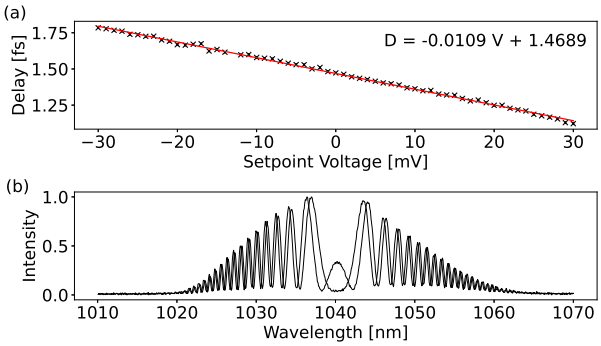

Fig. 4: The change in phase extracted from the spectra for varying set-point voltages in the PID loop driving the FS was converted to delay and plotted. The resulting fit gives a time calibration of 10.9 as/mV. The lower plot shows the maximum phase change over the set-point range –30 mV to +30 mV.

3 Results

To demonstrate long-term operation of the system, we ran a 24-hour test monitoring the spectrum and extracting the ZDW both with and without the stabilisation running. The results of this are summarised in Fig. 5. From this, a measurement of the peak-to-peak natural variation in delay between the two fibres over this period was 1.3 picoseconds. However, with the loops running not only was the ZDW unchanging, but the phase of the spectral interference remained locked.

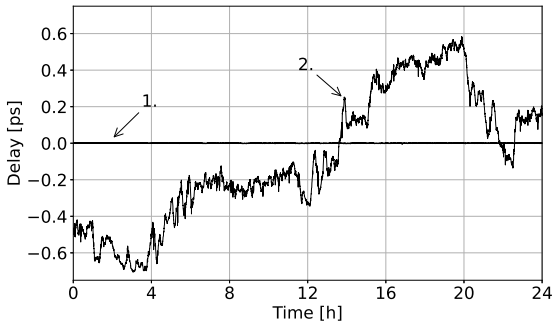

Fig. 5: 1. Over 24 hours we can see no drift at the picosecond scale to the system. 2. When unstabilised the delay between the fibres can be seen to change of the order of 1.3 picoseconds.

In order to better characterise the setup with the active stabilisation running, we performed three tests. First, a lock-in amplifier was used to input a signal into the loop at frequencies ranging from 10Hz to 40kHz and the attenuation of this signal was measured. In Fig. 6b we can see a high level of attenuation which linearly decreases up to higher frequencies. The line seen at 25 Hz is the known resonant line of the voice coil.

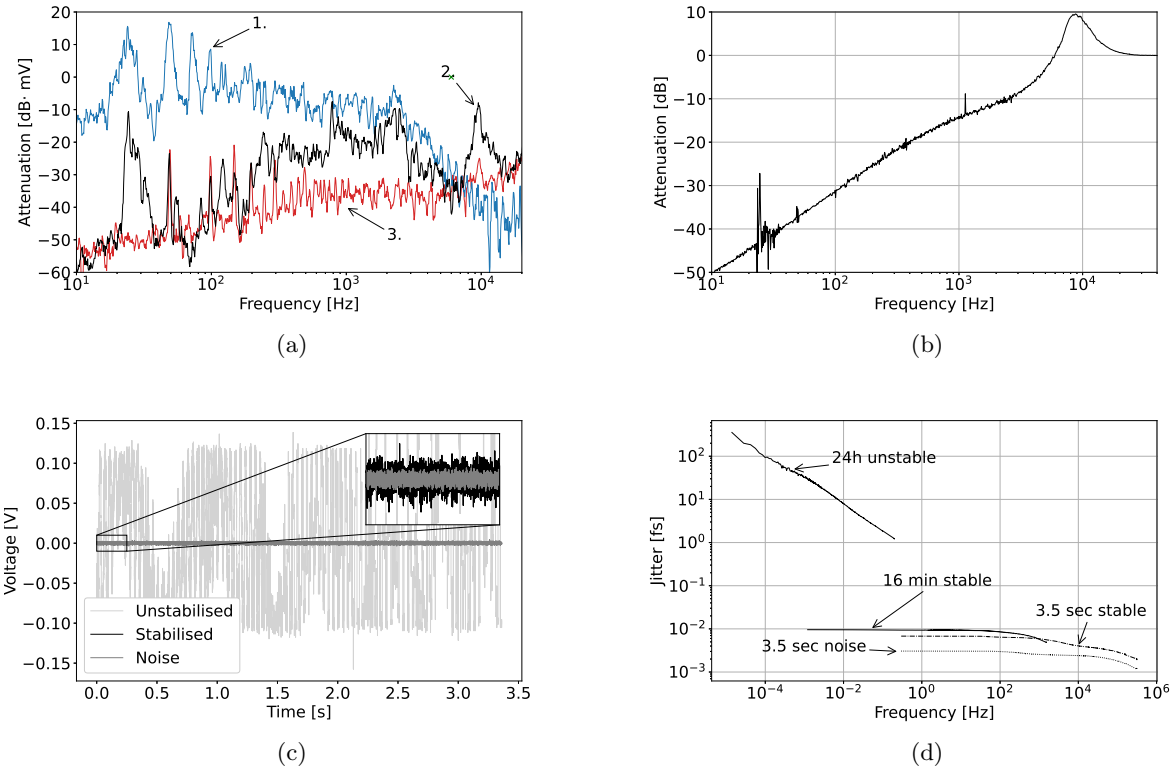

Fig. 6: (a) 1. Frequency amplitudes of the unstabilised signal 2. The attenuation of each frequency when the system is being stabilised 3. A measurement of the electrical noise of the sensor (b) Voltage output signal from the PSD over short time period of 3.5 s with 3.2 μs sampling interval. (c) Attenuation of a signal at each frequency. The spike at 25 Hz is a resonant line, known to come from the voice coil device (M1). (d) The integrated jitter up to the Nyquist frequency for the unstabilised, stabilised and noise signals. The total integrated jitter for the stabilised signal is 6.8 as.

Next, we measured the attenuation of the system for each frequency, for the three cases: stabilisation running, stabilisation off, and laser off to measure the electrical noise of the sensor. In practice, the measurements of unstabilised signals are really an underestimate of the true instability, as the fringe movement on the sensor is larger than the sensor itself. However, we can see in Fig. 6a the effectiveness of the stabilisation relative to the electrical noise of the sensor. Other than the resonant line at 25 Hz (due to the voice coil), which is suppressed but not eliminated, the stabilisation up to 100 Hz is indiscernible from the noise, which is an attenuation corresponding to a remarkable five orders of magnitude. For higher frequencies we still see suppression up to 6 kHz, with some amplification after this, consistent with the results seen in Fig. 6b.

For the final characterisation, we measured the total timing jitter for a single pass of the system. We took measurements of the voltage output of the PSD on a short time scale (3.5 seconds) with a sampling interval of 3.2 μs and medium time scale (16 minutes) with a sampling interval of 0.8 ms. Fig. 6c shows how close to the noise the system was capable of stabilising to. We then performed an integrated jitter calculation (Fig. 6d), giving the jitter up to a given frequency. Up to the Nyquist frequency we measure for the 3.5 second trace a total jitter in phase delay N_ϕ of 2.9 attoseconds, and for the 16 minute trace a total jitter of 6.8 attoseconds. As we are locking the phase, this jitter corresponds to the variation as a result of

the phase velocities in the recombined pulses. For a corresponding jitter in terms of the group delay N_g between the two pulses we use the following formula

$$N_g = \left(1 - \lambda \frac{\overline{n}'_f}{\overline{n}_f}\right)\Bigg|_{\lambda=\lambda_0} N_\phi \tag{8}$$

which is derived from relating the phase and group delays to the change in fibre path length. By assuming the mean refractive index of the fibre is fused silica, we yield the constant of proportionality in Eq. 8 to be very close to unity, and so the group delay jitter is actually indiscernible from the phase jitter.

We expect that these results will translate with larger fibre lengths and unwrapping the transport fibre, as this should only introduce low frequencies $\lesssim 100$ Hz from temperature and mechanical (vibrational) fluctuations which we have demonstrated this system is effective at suppressing.

4 Conclusion

In conclusion, we have demonstrated the suitability of spectral interferometry as an alternative technique applied to fibre-link stabilisation. We have exploited the advantages of linear techniques to construct a system capable of providing a stable timing signal to the next generation of experiments.

We have presented a robust method of detecting and compensating delay changes on the attosecond time scale with low power and uncompressed pulses, without the requirements of an ultra-stable oscillator source. This makes the this method potentially capable of delivering the precision of current systems at a mere fraction of the cost. The advantages of being able to measure delay in a large temporal window with a spectrometer also make this system easy to re-align when necessary.

Finally, although we see no fundamental limitation to extending this to a real world application, it will be interesting to see the effectiveness of obtaining a lock to a fringe which is moving by a larger magnitude on the 100 Hz scale and the task may not be so trivial. However with careful design considerations we believe this should be possible.

References

[1] Kumar, S., Parc, Y.W., Landsman, A.S., Kim, D.E.: Temporally-coherent terawatt attosecond XFEL synchronized with a few cycle laser. Scientific Reports **6**(1), 37700 (2016) https://doi.org/10.1038/srep37700

[2] Zastrau, U., Appel, K., Baehtz, C., Baehr, O., Batchelor, L., Berghäuser, A., Banjafar, M., Brambrink, E., Cerantola, V., Cowan, T.E., Damker, H., Dietrich, S., Di Dio Cafiso, S., Dreyer, J., Engel, H.-O., Feldmann, T., Findeisen, S., Foese, M., Fulla-Marsa, D., Göde, S., Hassan, M., Hauser, J., Herrmannsdörfer, T., Höppner, H., Kaa, J., Kaever, P., Knöfel, K., Konôpková, Z., Laso García, A., Liermann, H.-P., Mainberger, J., Makita, M., Martens, E.-C., McBride, E.E., Möller, D., Nakatsutsumi, M., Pelka, A., Plueckthun, C., Prescher, C., Preston, T.R., Röper, M., Schmidt, A., Seidel, W., Schwinkendorf, J.-P., Schoelmerich, M.O., Schramm, U., Schropp, A., Strohm, C., Sukharnikov, K., Talkovski, P., Thorpe, I., Toncian, M., Toncian, T., Wollenweber, L., Yamamoto, S., Tschentscher, T.: The High Energy Density Scientific Instrument at the European XFEL. Journal of Synchrotron Radiation **28**(5), 1393–1416 (2021) https://doi.org/10.1107/S1600577521007335

[3] Chekhlov, O., Collier, J., Clark, R.J., Hernandez-Gomez, C., Lyachev, A., Matousek, P., Musgrave, I.O., Neely, D., Norreys, P.A., Ross, I., Tang, Y., Winstone, T.B., Wyborn, B.E.: The 10 pw opcpa vulcan laser upgrade. In: CLEO/Europe - EQEC 2009 - European Conference on Lasers and Electro-Optics and the European Quantum Electronics Conference, pp. 1–1 (2009). https://doi.org/10.1109/CLEOE-EQEC.2009.5196350

[4] Rus, B., Bakule, P., Kramer, D., Korn, G., Green, J.T., Nóvak, J., Fibrich, M., Batysta, F., Thoma, J., Naylon, J., Mazanec, T., Vítek, M., Barros, R., Koutris, E., Hřebíček, J., Polan, J., Baše, R., Homer, P., Košelja, M., Havlíček, T., Honsa, A., Novák, M., Zervos, C., Korous, P., Laub,

M., Houžvička, J.: ELI-Beamlines laser systems: status and design options. In: Korn, G., Silva, L.O., Hein, J. (eds.) High-Power, High-Energy, and High-Intensity Laser Technology; and Research Using Extreme Light: Entering New Frontiers with Petawatt-Class Lasers, vol. 8780, p. 87801. SPIE, ??? (2013). https://doi.org/10.1117/12.2021264 . International Society for Optics and Photonics. https://doi.org/10.1117/12.2021264

[5] Dyer, G., Fry, A.: Matter in extreme conditions upgrade (conceptual design report) (2021) https://doi.org/10.2172/1866100

[6] Peng, M.Y., Callahan, P.T., Nejadmalayeri, A.H., Xin, M., Monberg, E., Yan, M., Grüner-Nielsen, L., Fini, J.M., Kärtner, F.X.: 1.2-km timing-stabilized, polarization-maintaining fiber link with sub-femtosecond residual timing jitter. In: CLEO: 2013, pp. 1–2 (2013). https://doi.org/10.1364/CLEO_SI.2013.CM4N.2 . ISSN: 2160-8989

[7] Ang, K.H., Chong, G., Li, Y.: Pid control system analysis, design, and technology. IEEE Transactions on Control Systems Technology **13**(4), 559–576 (2005) https://doi.org/10.1109/TCST.2005.847331

[8] Callahan, P.T., Safak, K., Battle, P., Roberts, T.D., Kärtner, F.X.: Fiber-coupled balanced optical cross-correlator using PPKTP waveguides. Optics Express **22**(8), 9749 (2014) https://doi.org/10.1364/OE.22.009749 . Accessed 2023-08-02